Journal of *Marine Science and Engineering*

MDPI

Article

Bottom and Suspended Sediment Backscatter Measurements in a Flume—Towards Quantitative Bed and Water Column Properties

Thaiënne A. G. P. Van Dijk [1,2,*,†], Marc Roche [3,†], Xavier Lurton [4,†], Ridha Fezzani [5], Stephen M. Simmons [6], Sven Gastauer [7,8], Peer Fietzek [9], Chris Mesdag [1,‡], Laurent Berger [5], Mark Klein Breteler [10] and Dan R. Parsons [6,§]

1 Department of Applied Geology and Geophysics, Deltares, 3584 BK Utrecht, The Netherlands; c.smesdag@freeler.nl
2 Department of Earth Science and Environmental Change, University of Illinois at Urbana-Champaign, Champaign, IL 61801, USA
3 Continental Shelf Service, FPS Economy, 1000 Brussels, Belgium; marc.roche@economie.fgov.be
4 Independent Researcher, 29280 Locmaria-Plouzane, France; xavier.lurton@orange.fr
5 Institut Français de Recherche pour l'Exploitation de la Mer (IFREMER), 29280 Plouzane, France; ridha.fezzani@ifremer.fr (R.F.); laurent.berger@ifremer.fr (L.B.)
6 Energy and Environment Institute, University of Hull, Hull HU6 7RX, UK; s.simmons@hull.ac.uk (S.M.S.); d.parsons@lboro.ac.uk (D.R.P.)
7 Thünen Institute for Sea Fisheries, 27572 Bremerhaven, Germany; sven.gastauer@thuenen.de
8 Scripps Institution of Oceanography, Integrated Oceanography, University of California, San Diego, CA 92037, USA
9 Kongsberg Discovery, 22529 Hamburg, Germany; peer.fietzek@kd.kongsberg.com
10 Department of Coastal Structures and Waves, Deltares, 2629 HV Delft, The Netherlands; mark.kleinbreteler@deltares.nl
* Correspondence: thaienne.vandijk@deltares.nl; Tel.: +31-6-5289-0378
† These authors contributed equally to this work and share first authorship.
‡ Presently retired.
§ Present Address: Geography and Environment, University of Loughborough, Loughborough LE11 3TU, UK.

check for updates

Citation: Van Dijk, T.A.G.P.; Roche, M.; Lurton, X.; Fezzani, R.; Simmons, S.M.; Gastauer, S.; Fietzek, P.; Mesdag, C.; Berger, L.; Klein Breteler, M.; Parsons, D.R. Bottom and Suspended Sediment Backscatter Measurements in a Flume—Towards Quantitative Bed and Water Column Properties. *J. Mar. Sci. Eng.* **2024**, *12*, 609. https://doi.org/10.3390/jmse12040609

Academic Editor: Philippe Blondel

Received: 19 February 2024
Revised: 21 March 2024
Accepted: 28 March 2024
Published: 31 March 2024

Abstract: For health and impact studies of water systems, monitoring underwater environments is essential, for which multi-frequency single- and multibeam echosounders are commonly used state-of-the-art technologies. However, the current scarcity of sediment reference datasets of both bottom backscatter angular response and water column scattering hampers empirical data interpretation. Comprehensive reference data derived from measurements in a controlled environment should optimize the use of empirical backscatter data. To prepare for such innovative experiments, we conducted a feasibility experiment in the Delta Flume (Deltares, The Netherlands). Several configurations of sonar data were recorded of the flume floor and suspended sediment plumes. The results revealed that flume reverberation was sufficiently low and that the differential settling of fine-sand plumes in the water column was clearly detected. Following this successful feasibility test, future comprehensive experiments will feature multi-frequency multi-angle measurements on a variety of sediment types, additional scatterers and sediment plumes, resulting in reference datasets for an improved interpretation of underwater backscatter measurements for scientific observation and sustainable management.

Keywords: multibeam backscatter; flume experiment; underwater habitat mapping; water column; suspended sediment plumes

1. Introduction

To understand the dynamics and resilience of the world's water systems, it is vital to monitor the development of their physical and ecological habitat characteristics. Acoustic systems have long been in use for measuring water depths and mapping subaqueous morphology. Moreover, measuring acoustic backscatter (i.e., echo intensities depending on the target intrinsic capability to return incoming acoustic energy after scattering as a

function of time or range [1]), single-beam (SBESs) and multibeam (MBESs) multi-frequency and broadband echosounders are the state-of-the-art technique for investigating both seabed interface [2–9] and water column [10] characteristics. For example, today's current applications of seabed interface characterization are the high-resolution mapping of seabed sediments for geoscience applications (the study of sedimentary processes and geological layering), hydrography, habitat characterization and monitoring [9] and ecology. Water column applications mainly focus on detecting biotic targets of the pelagic ecosystem, ranging from zooplankton to fishes and marine mammals [11–13] and on monitoring abiotic targets, such as suspended sediment plumes [14,15] and gas seepage [16], and fluid expulsion [17] from the seabed. Furthermore, acoustic backscatter can profitably be applied to investigate submerged archaeological sites [18]. Beyond imaging these various targets, echosounder data can provide quantitative information on target properties through quantitative measurements of the backscatter signal, made possible by calibration procedures [19]. Backscatter calibration is nowadays a routine procedure for SBESs, using a known reference target, and allows for the evaluation of acoustic system constants, giving absolute values of volume or surface backscatter strength under certain hypotheses. In addition, dedicated high-frequency, narrow-beam acoustic backscatter systems (ABSs) are available for measuring backscatter profiles in the water column; they are calibrated on targeted controlled sediments for both the acoustic system and sediment constants, giving access to sediment concentration and grain size. However, calibration is still exploratory for MBESs [20,21].

Calibrated MBES backscatter (BS) measurements provide absolute amplitudes of the target strength of seafloor insonified areas, offering the great advantage of spatial and temporal comparability. However, due to the technical difficulty of ensuring MBES calibration, a large part of MBES BS data acquired in underwater geosciences are still derived from uncalibrated systems, making them usable only in relative mode under restrictive conditions, as, for example, in the framework of BS time series analysis [22,23]. Consequently, the geoscientific interpretation of BS data requires reference data. Most reference values available today come from either modeling (e.g., theoretical angular response curves of generic sediment types; [24]) or from at-sea experiments over complex, natural beds (e.g., sediment heterogeneity, interface roughness, layering, shell content, vegetation, and sediment disturbance by living organisms [8]), further complicated by the influence of seasonality [9], survey conditions [5] and the difficulty of adequate validation by ground-truthing [8]. Moreover, BS levels for coarser sediments were found to be ambiguous [25]. This combination of complexities makes field results hard to reduce to canonical configurations. For suspended sediment plumes, calibrated ABS measurements allow for deriving sediment concentration and grain size in the water column, but the relation between BS measured by SBES/MBES and sediment plume properties is still largely unexplored. Therefore, the interpretation of empirical BS measurements of both the bed and water column would best be served by validation using reference values over a wide range of sediments, sonar frequencies and beam incident angles, as obtained from well-controlled experimental works [7,26]. However, only a few ex-situ (in-tank) measurements of the angular and frequency dependency of BS levels for realistic sedimentary targets have been conducted [27–31], mainly explained by the practical difficulties involved in such experiments.

Working at moderate sonar frequencies (as low as tens of kHz) and shallow grazing angles for measuring several types of bed sediments and in-water plumes raises acoustical and geometrical constraints for an experimental set-up, requiring a sufficiently large facility in which natural sediments may be used in sufficient quantities. The Delta Flume (291 m long, 5 m wide and 9.5 m deep for an actual maximum water depth of 9 m; see Materials and Methods; [32]) of Deltares, Delft, The Netherlands, is a well-adapted infrastructure for conducting such large-scale, systematic reference measurements of both floor and suspended sediment backscatter at various frequencies (the ones typically used by current echosounders) and beam angles, under controlled conditions in terms of the following:

- Bed sediment type and grain size distribution;
- Water–sediment interface roughness and physical configuration (ripples; heterogeneous scatterers, such as shells, gravel, or seagrass);
- Sediment thickness and layering;
- Sediment plume composition and behavior (particle size distribution, plume shape dynamics and concentration).

Preliminary theoretical calculations of echosounder "footprints" on the flume floor (i.e., areas defined by the intersection of the sonar beam with the targeted interface [1]) were conducted for various configurations of altitude and beam tilt angle; this analysis showed that all the beam widths (7° and 16° for the SBES, and 5° for the MBES) fit the Delta Flume dimensions well. However, we anticipated that the flume's relative narrowness (5 m) could still induce unwanted reverberation levels prone to mask the expected target echoes; indeed, the risk of sonar measurements in such a confined space is that the echoes from the flume walls are recorded through the sidelobes of the echosounder beams [33] and are mixed with the expected signals, contrarily to the ideally desired conditions of a "free-field" (i.e., where no obstacle can cause unwanted echoes interfering with the expected measurement). Before designing a large-scale project of in-flume measurements, we deemed it necessary to evaluate the risks of perturbed backscatter measurements with currently available echosounders by the acoustical response of the flume itself (mainly discrete multiple echoes from the walls, floor and in-water obstacles and additive noise, either electrical or acoustical).

This paper presents the design, outlines of operations and results, and discusses the findings of this feasibility experiment aimed at (1) testing the flume reverberation for various geometrical and acoustical configurations (e.g., varying transducer depths, using different frequencies and beam angles) by conducting acoustic measurements in real size and under realistic conditions of target properties (floor and plumes) with representative sonar systems and (2) the processing and quality assessment of these data, in view of the future comprehensive experiments. Even though this feasibility study was focused on the fundamental acoustical and methodological aspects, the set-up and scientific results are of significance to the wider scientific community.

2. Materials and Methods

2.1. Experimental Design

This feasibility study was designed to test reverberation levels within the Delta Flume (Figure 1(1)), conducting real-size, real-time acoustic measurements for a large number of configurations of different sonar altitudes, frequencies, and beam angles, with contemporary acoustic equipment. The test was realized in a compartment of the flume (Figure 1(1,2)).

2.2. Acoustic Systems

The Simrad EK80 (Kongsberg Discovery AS, Horten, Norway) is a multi-frequency, single-beam, split-beam echosounder [34] used as the reference instrument for this experiment. Thanks to its capability of being calibrated for angular intensity measurements [19], it can provide an absolute level of backscatter strength for point-like, surficial or volume targets. Its narrow single-beam structure (7° beamwidth at −3 dB) provides very low levels of sidelobes with two-way rejection rates better than −50 dB. Available transducers supported by the broadband transceiver cover a wide frequency band (34–450 kHz). The system operated in this project featured three transducers at nominal frequencies of 70, 200 and 333 kHz.

The EM2040c (Kongsberg Discovery AS, Horten, Norway) is a portable, multi-frequency MBES designed for shallow-water operations [35]. At 300 kHz, the nominal transmission sector aperture is 1° × 150°, with 1°-wide beams formed in reception. A Seapath 130 GPS (Kongsberg Discovery AS, Seatex, Trondheim, Norway), with an MRU5 motion sensor [36], was connected to the EM2040c to include constant position and motion data

in the datagrams. Like most MBESs, the EM2040c cannot be calibrated as conveniently as an SBES; the most practical way is to cross-calibrate it with calibrated SBES BS levels on a common target [21].

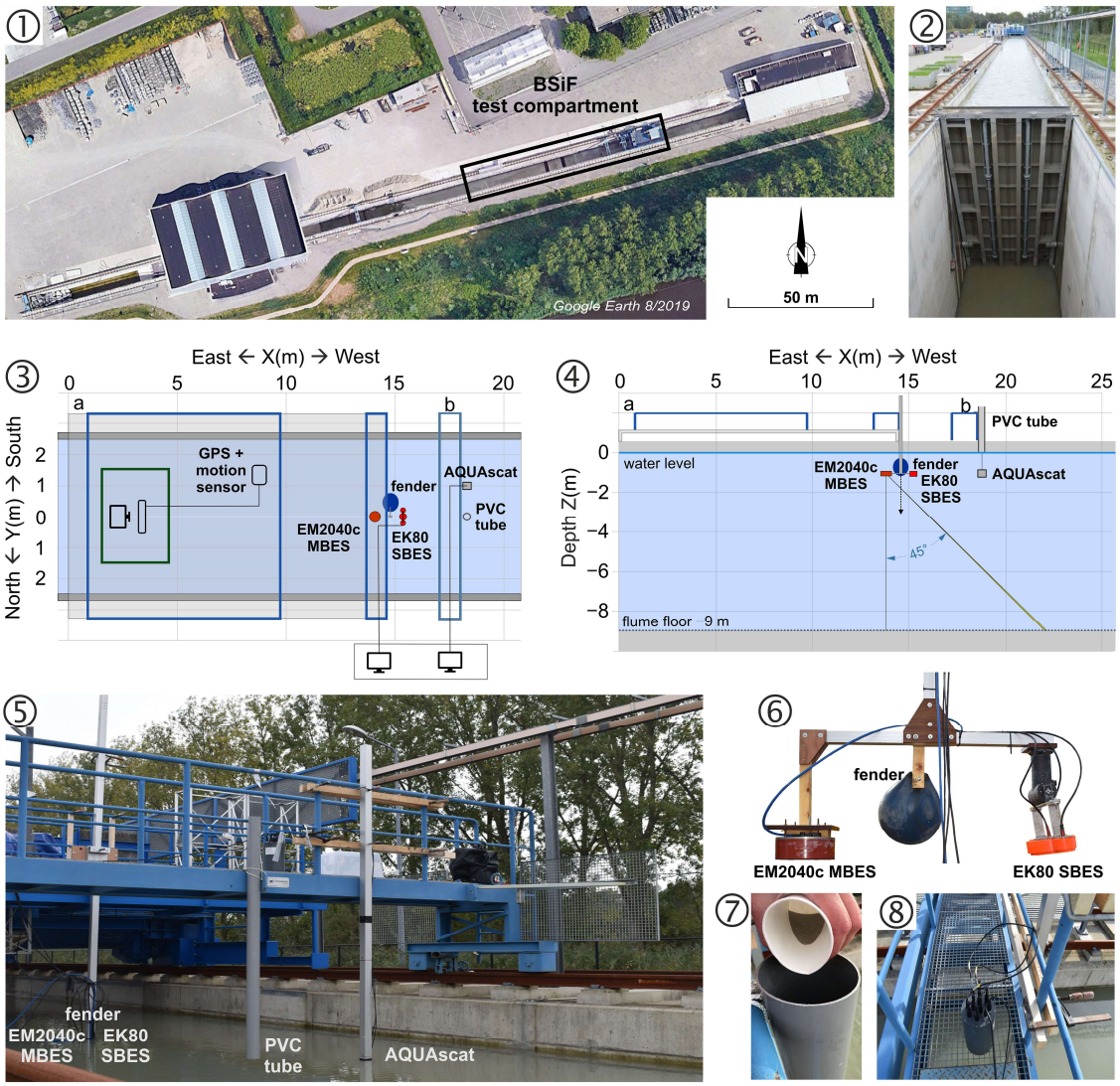

Figure 1. The Delta Flume and experimental set-up. (**1**) An overview of the flume with the location of the test compartment. (**2**) The compartment wall in the Delta Flume with a water height of 9 m. (**3**) The installation plan of the equipment (top view); (**a**) the measuring trolley spanning the flume width and riding over along-flume rails; (**b**) the mobile bridge. (**4**) The installation plan of the equipment (longitudinal cross section; same legend as (**3**)). (**5**) An overview of the equipment installed in the Delta Flume. (**6**) The height-adjustable pole-end structure supporting the EM2040c transducer, the fender and the EK80 transducers mounted below the pan-and-tilt unit. (**7**) Pouring a 20 g sand sample into the PVC tube. (**8**) The AQUAscat receiver next to its pole.

An AQUAscat (Aquatec Group, Basingstoke, UK) acoustic backscatter system [37] was deployed as a calibrated reference, capable of profiling suspended sediment plumes through the full water column of 9 m, using three transducers with frequencies of 0.99, 1.85 and 4 MHz; however, only the two lower ones proved to be usable. Due to this very high frequency range, the purpose was not to compare these acoustic echoes with the SBES/MBES data recorded at lower frequencies but to provide an independent source of validation for sediment concentration during the plume experiments.

2.3. Equipment Installation in the Delta Flume

The sonar equipment was installed on the main mobile measuring trolley (see Figure 1(3–8)). The dry-end components and ancillary devices were sheltered either on the trolley platform (EM2040c) or on the flume quay (EK80 and AQUAscat). A smaller mobile bridge hosted the provisional plume generator and the AQUAscat.

The sonar heads were fixed at the lower tip of a dedicated, vertical and extending pole, deployed in the across-flume center and off the side of the main trolley platform, allowing for immersions at varying depths down to 8 m with a water height of 9 m. For the EK80 to record echoes at various tilt angles, its transducers were fixed on a SS250 pan-and-tilt device (SIDUS, San Diego, CA, USA) [38], digitally controlled from the flume quay (Figure 1(3)). A calibration sphere (38.1 mm tungsten carbide with 6% cobalt binding) was located at 5.5 m depth and 5 m from the MBES. The EM2040c head was fixed with the wide aperture of the transmit sector oriented along the flume length; no tilt was applied to the transducer array, since the 256 formed beams provide the necessary angular scanning. The AQUAscat was installed 1 m south of the across-flume center at a fixed level, 1 m below the water surface (i.e., 8 m above the floor; Figure 1(4)).

To generate sand plumes in the water column in a controlled and repeatable way, a PVC tube was installed on the smaller mobile bridge, 1 m north of the AQUAscat and in line with the EK80 and EM2040c, with the tube outlet just above the water level (Figure 1(5,7)).

2.4. Measurement Operations

The experiment was conducted on 12–15 October 2020. A limited 70 m long compartment of the Delta Flume (Figure 1(1)) was sufficient to record floor echoes at incident angles as oblique as 75° and was physically delimited in this respect (Figure 1(2)). The water depth in the compartment was 9 m. From an acoustical point of view, the most constraining feature of the Delta Flume is its width of 5 m between the two walls, prone to generate strong echoes at very short delays.

For the flume floor measurements, the EK80 was operated at 3, 4, 6 and 8 m above the floor, with transducers at nominal frequencies of 70 and 200 kHz (respective bandwidths 45–90 kHz and 160–260 kHz) and—for each altitude—at beam tilt angles of 0°, 30°, 45°, 60° and 75°. The EK80 transmitted power was 150 W at 70 kHz and 90 W at 200 kHz (i.e., respectively, 220 and 217 dB re 1 µPa at 1 m), using several pulse lengths. At the same depths, the EM2040c was operated for full-swath coverage at frequencies of 200, 300 and 400 kHz, using several pulse lengths per frequency. Floor echoes were recorded for 1 min per configuration at five pings per second. No sediment was spread on the flume floor for this feasibility experiment; hence, the echoes were generated by the concrete floor (with a thin residual mud layer from an earlier flume operation).

The flume was filled with fresh water; the hydrological parameters proved to be stable over depth and time (Text S1; Figures S1 and S2).

For the plumes, an industrial 0/2 certified marine sand was dried and pre-sieved to create well-sorted subsamples of five granulometric fraction ranges: 63–125, 125–180, 180–212, 212–250 and 250–500 µm. The sand plumes were generated by pouring varying sand samples into the dedicated tube (Figure 1(7); Video S1). A first set of plumes comprised the same grain size (fine sand; 180–212 µm) and varying total masses of sediment (3, 15, 37, 70 and 300 g per plume), thereby varying sediment concentration. A second series of plumes comprised a constant sediment mass (20 g) for the four coarsest sand fractions. Series of simultaneous EK80, EM2040c and AQUAscat recordings were made of the plumes at 8 m altitude during the full settling time (on average 7 min). The EK80 was operated with transducers at nominal frequencies of 200 and 333 kHz (160–260 kHz and 260–450 kHz bandwidths; the transmitted power at 333 kHz was 50 W or 212 dB re 1 µPa at 1 m) and tilted at 25° or 45°. For the EM2040c, we recorded the first set of plumes at 300 and 400 kHz and the second set at 400 kHz, both with a 25 µs pulse length. Using the mobile bridge (Figure 1), the distance of the sand tube to the EM2040c array was adjusted to intercept the sand plumes at oblique incidence angles between 30° and 50° at 300 kHz and

between 15° and 35° at 400 kHz. The AQUAscat, looking near-vertically down onto the plumes, recorded water column backscatter profiles, using three transducers with acoustic frequencies of 0.99 MHz, 1.85 MHz and 4 MHz. Using 110 measurement cells of size 80 mm gave a profiling range of 9.16 m extending beyond the range to the flume bottom for the two lower frequencies. A pulse repetition frequency of 10 Hz was used as this was the instrument's highest rate for the given cell size and profile range, and averaging was performed over groups of eight consecutive profiles before data were recorded by the instrument.

2.5. Data Analysis

The EK80 raw data were corrected for the echosounder calibration offsets and the water absorption; the backscatter strength values were then computed according to the standard methods presented in [19]. The echoes from the flume floor and walls (Figure 2) were processed and analyzed using interface backscatter modeling [1,21]. For the sediment plumes (Figure 3), the data were analyzed using the volume backscatter model [1,19].

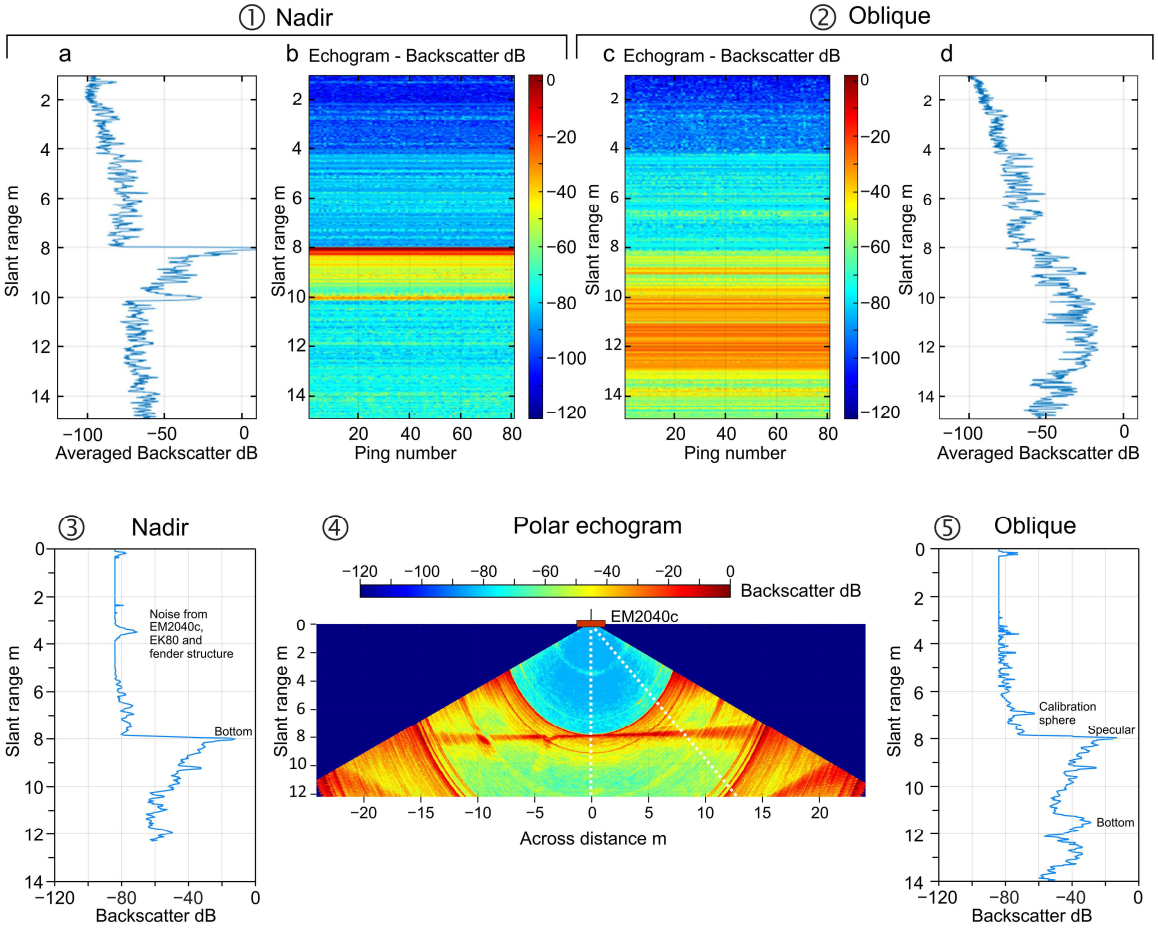

Figure 2. Classical presentations of bottom echoes from run with sonar altitude of 8 m above flume floor. (**1**,**2**) EK80 data at 200 kHz with 128 µs pulse length. (**1**) Nadir, 0° angle: (**a**) averaged backscatter versus slant range (i.e., average echo amplitude for all pings in time series on *x*-axis vs. time in reception on *y*-axis; at vertical, slant range is equivalent to depth below sonar head); (**b**) echogram (BS intensities [dB] in time series [ping number] vs. slant range); and (**2**) oblique, 45°-tilted angle: (**c**) echogram; and (**d**) averaged backscatter versus slant range. (**3**–**5**) EM2040c at 200 kHz with 25 µs pulse length. (**3**) Single-ping from isolated 0° beam: backscatter versus slant range; (**4**) polar echogram, i.e., vertical cross-cut of water column and floor BS for one ping; (**5**) single ping from isolated 45° beam, backscatter versus slant range. On all plots, "Backscatter dB" quantity is backscattering strength computed in the case of interface reverberation process [21].

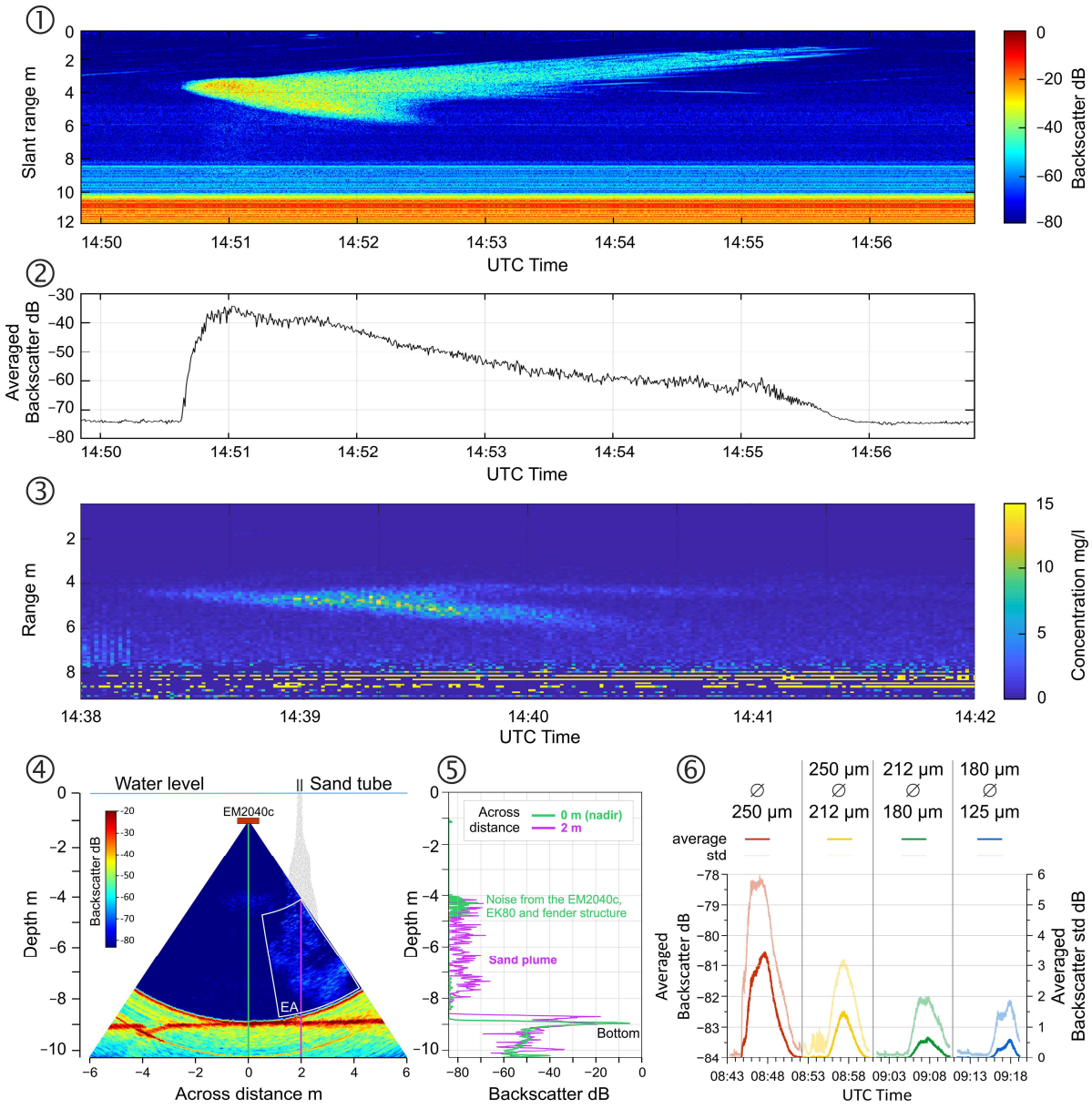

Figure 3. EK80, AQUAscat and EM2040c sand plume backscatter records in the water column. (**1**–**5**) For a sand plume of 300 g with 180–212 µm grain size. (**1**,**2**) EK80 data at 45°-tilt, 200 kHz with a 128 µs pulse length. (**1**) Backscatter echogram. (**2**) Sv (volume backscatter strength) averaged over the free water range (i.e., oblique range up to 8 m). (**3**) AQUAscat inverted backscatter shows plume sediment concentrations in mg/l for the 1.85 MHz transducer. (**4**–**6**) EM2040c data at 400 kHz with a 25 µs pulse length. (**4**) Polar echogram example. (**5**) Backscatter intensity versus the depth of two vertical lines shown in (**4**), at nadir (green) and at a 2 m across distance (purple); the signal generated by the plume is clearly quantifiable. (**6**) The echo integration of four 20 g plumes of different grain size fractions. Considering the echo integration area (EA) shown in (**4**) and the 1° beam width, the insonified water volume is approximately 1 m^3. BS mean values and standard deviations (stds) are estimated for each ping and plotted versus UTC time.

The EM2040c data were processed using the SonarScope® software suite [39]. For the echoes from the flume floor and walls (Figure 2), the echograms presented here are gridded representations of the BS values, from which individual beam angles can be resampled (Figure 2(3,5)). For the analyses of sediment plumes, a qualitative (i.e., uncalibrated) volume backscatter strength was used, as calculated according to Equation 9 in [40]. The echo

integration was processed inside a water volume defined by an angular sector and a slant range interval in the across-track plane ("EA" area drawn in Figure 3(4)) and the MBES beamwidth in the along-track direction. The proper selection of this area isolates the plume BS values from unwanted echoes caused by, e.g., the fender.

The post-processing of the AQUAscat backscatter data followed the implicit iterative method [41] that made use of a grain size distribution measured with a Malvern and transducer calibration constants measured in a sediment tower [42]. The raw backscatter data were corrected for spherical spreading and water absorption using the formulae of [43,44], and the scattering and attenuation properties of the sand were derived using the heuristic formula of [45]. A first inversion for sediment concentration was used to determine the sediment attenuation along each profile, updating the concentration profiles through 10 iterations until the attenuation-adjusted concentration profiles converged.

3. Results

During this feasibility study, various geometrical and acoustic configurations were tested for the deployment of sonar systems in the Delta Flume; in all cases, it was found that for sonar altitudes from 3 to 8 m above the floor, the strong echoes from the flume floor clearly dominated unwanted echoes from the flume walls, both for SBESs and MBESs. Suspended sediment plumes of different sediment masses, from 300 g down to 3 g of sediment in a 9 m water column, were clearly detected in the backscatter measurements at higher frequencies of 200, 300 and 400 kHz, depending on the plume concentration. Validation with the separate ABS measurements allowed for a comparison of the water column SBES and MBES backscatter levels with the water column profiles of the inverted sediment concentration. Time series revealed the plume dynamics and segregation of grain sizes during the plume settlement.

3.1. Echoes from Flume Floor and Walls

3.1.1. SBES

From the various altitude/tilt angle/frequency configurations as recorded in EK80 time series, Figure 2(1,2) show exemplary results of measurements at an 8 m echosounder altitude at 200 kHz. The 'Backscatter' quantity plotted here is the interface backscattering strength [21] that has been extracted from the recorded echo amplitudes corrected under the hypothesis of interface backscattering. The vertical incidence recordings (0°, at the nadir) display strong echoes from the flume floor, mixing a specular reflection phenomenon with the interface backscattered contribution (leading to a computed BS peak value higher than 0 dB at 8 m in Figure 2(1)). Considering the geometry of the flume, the first sidelobe contribution (BS intensities of ca. −100 to −80 dB around 2.5 m depth in Figure 2(1)) corresponds to direct reverberation from the flume wall at 2.5 m and is actually weak, thanks to sidelobe rejection. The first significant sidelobe (at 30° from the vertical) hits the wall at a distance of approximately 4 m (BS levels of ca. −80 to −60 dB). High BS intensities (−50 to −40 dB) directly following the main peak are due to the beam width, giving later returns for the outer area around the central axis of the main lobe, as well as sidelobe contributions. The double echo (ca. −28 dB at 10 m) is due to the bottom—water surface—echosounder multipath echo. For the oblique 45° tilted beam (Figure 2(2)), echoes from the flume floor (at an 11.3 m slant range) occur between 10 and 13 m, the spreading being due to the returns of echoes from the outer parts of the main beam. The increased BS values (−60 to −40 dB) at 8 to 10 m correspond to the first return of the flume floor (the vertical echo through sidelobes).

We found that in all the time series, including other configurations not shown here, the flume bottom echoes strongly emerged from the background noise and flume reverberation (up to an 80 dB contrast at the vertical and approximately 25 dB contrast at a 60° steering angle). To conclude this SBES data analysis, although the unwanted specular echoes from the side walls could clearly be geometrically identified on the recordings, they did not cause significant interference prone to perturb the measurements of flume floor echoes.

3.1.2. MBES

With the MBES swath length oriented in the along-flume direction (i.e., the polar echogram of Figure 2(4) corresponds to the vertical plane along the channel axis), it was possible to record full swath echoes, including shallow-grazing incidences. The flume floor echo observed at the nadir shows a high intensity level (−12 dB at an 8 m depth in Figure 2(3,4)), well above any measured noise level. At −4 m and −9 m along the flume axis, two across-flume grooves can be observed (Figure 2(4)). For the oblique beam (45°; Figure 2(5)), a strong specular echo is seen at 8 m, and the flume floor echo is distinct (at an 11.3 m slant range); the weak echo (−62 dB) at a 7 m slant range is caused by the calibration sphere. The main perturbation in the measurements comes from the well-known "specular circle" [46], generated by the reflected signal at normal incidence and insufficiently rejected by the oblique receiving beams; note that this effect is inherent to all MBES systems and usually does not prevent adequate measurements at oblique incidences. No significant contribution was observed from the flume walls, meaning that the "along" directivity rejection of the sidelobes is sufficient.

Although the quality of the oblique incidence backscatter measurements is not as good as those obtained by the EK80 SBES, the in-flume MBES results are consistent with data expected under free-field conditions during at-sea or in-river measurements.

3.2. Suspended Sediment Plume Echoes in the Water Column

Suspended sediment plumes entered the insonified areas of the SBES and MBES when gravitating down to the flume floor (see Figure 3). The ABS located in the proximity of the sediment tube insonified near-vertically down onto the plumes.

3.2.1. SBES

All the EK80 SBES results show that the plume-backscattered echoes emerge with a good contrast from the background noise and flume reverberation. In the case of a sand plume of 300 g with 180–212 µm grain size (Figure 3(1,2)), strong averaged BS intensities of up to −35 dB were recorded when the plume entered the insonified area of the 45° beam, compared to a water column background BS level of −75 dB (Figure 3(2)). In the time series, the downward-shifting BS intensities in Figure 3(1) exhibit the gravitating down of the sediment plume, which disappears from the 45° beam insonified area after ca. 2 min; the upward-moving BS intensities likely represent air bubbles surfacing after being released from sediment grains or shell fragments. The flume floor echoes are visible at 8 m (weak vertical echo through sidelobes) and 10–12 m (main lobe). Note that the quality of the results (i.e., the reverberation level) depends on the frequency considered (better results at higher frequencies due to the scattering properties of the sand plume) as well as on the sediment concentration. Even the lowest sediment load (3 g total mass) proved to be well detected at 300 kHz and above.

3.2.2. ABS

The backscatter from sediment plumes was successfully recorded by AQUAscat for the two lowest frequencies. The 4 MHz frequency may have been too high for penetrating the plumes and/or water column, and its results were not considered. Figure 3(3) shows sediment concentrations up to 10–15 mg/liter for the 1.85 MHz frequency of a 300 g plume of 180–212 µm sand. Similar concentrations are seen for both the 0.99 and 1.85 MHz frequencies, which adds confidence that the measurements are well constrained. The signal-to-noise ratio is visibly poorer near the flume bed, but the sediment plume extent is consistent between the two transducers, demonstrating that the AQUAscat provides a useful means of quantifying suspended sediment concentrations over the 8 m range down to the flume bottom.

3.2.3. MBES

All generated plumes were detectable on the EM2040c echograms recorded at 300 kHz and 400 kHz. The 300 g plume with 180–212 µm grain size at 400 kHz is illustrated in Figure 3(4) and Video S2. Suspended fine-sand grains generate a backscatter level of 10 to 15 dB higher than the −84 dB threshold background level. The plume-related amplitudes are at the same level as the unwanted echoes from the fender (Figure 3(5), installed for easy adjustment of the sonar head height), which was identified by its geometric location. The echo integration of the plume backscatter data reveals that the average backscatter level in the insonified water volume correlates with the grain size variation for plumes of constant weight (Figure 3(6)) and with the variation in sediment weight for the same grain size (not shown here). If only a portion of a plume passes through the insonified water volume, the EM2040c is still capable of detecting a plume of fine sand with concentrations less than 20 mg/L. For comparison, but without considering grain size, 20 mg/L is the order of magnitude of the lowest suspended particulate matter concentration (SPMC) recorded offshore in the Belgian part of the North Sea, while in turbid coastal areas, thte SPMC exceeds 100 mg/L [47,48]. The dynamic visualization of the plume echograms (Video S2) reveals horizontal displacements of the plumes, suggesting the presence of weak currents within the flume.

4. Discussion

The results obtained from this backscatter-in-flume feasibility experiment constitute a rich and informative dataset and validate the achievability of controlled acoustic measurements in the Delta Flume. In some respects, considering their diversity and their metrological quality, these results exceed the initial objective of a feasibility check.

4.1. Bed and Plume Detection

The sufficient contrast of backscatter intensities of echoes from both the flume floor and the suspended sediment plumes with respect to background backscatter levels evince that backscatter measurements are not masked by reverberation. For both SBESs and MBESs, the geometrical configurations provide reliable measurements at all considered incident angles (up to 75° for the EK80 and 70° for the EM2040c). Herein, the results are of the highest quality for the SBES (thanks to its excellent sidelobe rejection) and less so for the MBES, which, however, was revealed to still be satisfactory for both bottom and plume backscatter measurements. The separate high-frequency backscatter from the AQUAscat corroborates the reliability of the suspended sediment plume measurements and justify to link the sonar backscatter intensities with the sediment concentration and grain size.

Although the MBES used here was not previously calibrated, its recorded echoes are readily compared to calibrated EK80 echoes on the same targets in the same configuration. This allows for cross-calibration as used for at-sea measurements [21] and hence gives access to standardized absolute values of the backscatter strength needed for building a reference database.

4.2. Suspended Sediment Plume Concentration, Grain Size and Dynamics

The sediment plume results illustrate a correlation between the inserted weight (equivalently, the sediment concentration in the plume) and the particle size distribution on the one hand and the water column backscatter intensities on the other (see Figure 3(6)). In particular, the results confirm the ability of echosounders to detect very low concentrations of fine sand: even a plume of only 3 g of fine sand can be distinguished from the water column background backscatter mean level. Compared to the 300 g plume sediment concentrations (AQUAscat 10–15 mg/L; Figure 3(3)) and sediment concentrations in turbid coastal environments (>100 mg/L), the successful detection of the 3 g plume is promising.

During the gravitating down of the plumes, the echosounder time series reveal changes in the plume shape. The horizontal widening of the plume is consistent with sediment plume dynamics due to water resistance during the development of the plumes [49]. The

observed lengthening of the plume in the vertical direction exhibits the segregation of grain sizes, where the larger grain size fractions gravitate faster than the smaller grain size fractions. Although the upward-moving tail of the plume's BS intensities (in Figure 3(1); likely caused by the gradual release of air bubbles trapped by sediment grains) could ideally be avoided in such experiments, these may also represent naturally or anthropogenically induced suspended sediment plumes [50] and may provide information about plume behavior.

5. Perspectives

For the sustainable use of underwater environments, habitat mapping as well as monitoring anthropogenic impacts require an improved interpretation of backscatter measurements of natural seabed and water column properties. To answer the need for calibrated backscatter reference measurements in a controlled environment, the authors are designing a large-scale experiment in the Delta Flume that includes analyses of frequency and incident angle dependency (for both SBESs and MBESs, over large ranges, closely sampled) for a wide range of sediment types and suspended sediment plumes (see Introduction). For bottom backscatter, different configurations of sediment grain size and sorting, seabed roughness, densities of additional scatterers (clasts, shells, seagrass) and sub-surface layering will be realized on the flume floor. For the suspended sediment plumes, a dedicated sediment-pouring device will be developed to obtain given flux values and plume geometries in a reproducible way. The various plume concentrations and grain size distributions will be linked to the echosounder backscatter data, using calibrated high-frequency measurements of the AQUAscat.

Besides the original main goal of feasibility validation, the tangible results presented here confirm the relevance of the principle of in-flume backscatter measurements of sedimentary seafloor and plumes. The results of this preliminary test act as proof of concept, and the lessons learned provide a solid basis for the improved design and operations of the comprehensive future experiments, leading to defined backscatter reference models for the improved interpretation of underwater habitat mapping.

Building a database of reference angular response curves, parameterized by the sediment properties and acoustic configurations, jointly with developing heuristic backscatter strength models, will improve the interpretation capability for both bed interface characteristics and in-water suspended sediment plumes. To further validate and add to the reference models resulting from the in-flume experiments, such experiments will have to be completed by field studies in contrasting natural environments, including coastal habitat mapping for biodiversity, ocean observation for deep-sea geological exploration and the monitoring of industry-related activities, such as dredging and nourishing in rivers and shallow seas.

The resulting reference models will impact many backscatter users (industry, governmental agencies, hydrography and ocean sciences) active in geological and ecological subjects, in deep and shallow marine, coastal, fluvial and lacustrine environments worldwide.

Supplementary Materials: The following supporting information can be downloaded at: https://www.mdpi.com/article/10.3390/jmse12040609/s1.

Author Contributions: All authors have contributed to the research and writing of this paper. Conceptualization, T.A.G.P.V.D., M.R. and X.L.; methodology, T.A.G.P.V.D., M.R., X.L., R.F., S.M.S., S.G., P.F., L.B., M.K.B. and D.R.P.; investigation, flume measurements, T.A.G.P.V.D., M.R., R.F., S.G., C.M. and M.K.B.; analyses, validation, M.R., R.F. and S.M.S.; writing—original draft: T.A.G.P.V.D., M.R., X.L., R.F., S.M.S. and P.F.; writing—review and editing: T.A.G.P.V.D., M.R., X.L., R.F., S.M.S., S.G., P.F., C.M., L.B., M.K.B. and D.R.P.; visualization: M.R., R.F. and S.M.S.; supervision: T.A.G.P.V.D., M.R., X.L., L.B. and D.R.P. All authors have read and agreed to the published version of the manuscript.

Funding: This feasibility experiment was funded by substantial in-kind contributions for facilities, equipment, research time and expenses from Deltares, FPS Economy, Xavier Lurton, Ifremer, University of Hull and Kongsberg Discovery (KD). This research was financed by Deltares (58%), FPS Economy, Belgium (21%) and Rijkswaterstaat (RWS, 21%).

Institutional Review Board Statement: Not applicable.

Informed Consent Statement: Not applicable.

Data Availability Statement: In support of the findings and conclusions in this paper, multibeam echo soundings (MBES, EM2040c), single-beam echo soundings (SBES, EK80) and acoustic backscatter system data (ABS, AQUAscat), as recorded in the Delta Flume in 2020, as well as their configurations, are available on SEANOE [51]. Tables explaining the available datasets, their configurations and equipment are given in the repository. The EM2040c data were analyzed with SonarScope software [39]. Data are Open Access under the licensing Creative Commons Attribution 4.0 International (CC BY 4.0, https://creativecommons.org/licenses/by/4.0/, accessed on 20 March 2024).

Acknowledgments: The on-site experiments were assisted by John Coolegem, Frank van Eden and Danny van Doeveren (Deltares Flume crew), Kevin Weerman (KD Netherlands) and Simon Bicknese (RWS) and were further supported by Lars Nonboe Andersen and Kjetil Jensen (both KD Norway). The marine sand for the plume experiments was provided by De Cloedt, Belgium.

Conflicts of Interest: The authors declare no conflicts of interest.

References

1. Urick, R.J. *Principles of Underwater Sound*, 3rd ed.; McGraw-Hill: New York, NY, USA, 1983.
2. Hughes Clarke, J.E. Optimal Use of Multibeam Technology in the Study of Shelf Morphodynamics. In *Sediments, Morphology and Sedimentary Processes on Continental Shelves*; Li, M.Z., Sherwood, C.R., Hill, P.H., Eds.; Wiley: Hoboken, NJ, USA, 2012; pp. 1–28.
3. Hughes Clarke, J.E. Multibeam Echosounders. In *Submarine Geomorphology*; Micallef, A., Krastel, S., Savini, A., Eds.; Springer: Berlin, Germany, 2018; Chapter 3; pp. 25–41.
4. Gaida, T.C.; Tengku Ali, T.A.; Snellen, M.; Amiri Simkooei, A.; Van Dijk, T.A.G.P.; Simons, D.G. A multispectral Bayesian classification method for increased acoustic discrimination of seabed sediments using multi-frequency multibeam backscatter data. *Geosciences* **2018**, *8*, 455. [CrossRef]
5. Gaida, T.C.; Van Dijk, T.A.G.P.; Snellen, M.; Vermaas, T.; Mesdag, C.; Simons, D.G. Monitoring underwater nourishments using multibeam bathymetric and backscatter time series. *Coast. Eng.* **2020**, *158*, 103666. [CrossRef]
6. Brown, C.J.; Beaudoin, J.; Brissette, M.; Gazzola, V. Multispectral Multibeam Echo Sounder Backscatter as a Tool for Improved Seafloor Characterization. *Geosciences* **2019**, *9*, 126. [CrossRef]
7. Montereale-Gavazzi, G. Development of Seafloor Mapping Strategies Supporting Integrated Marine Management—Application of Seafloor Backscatter by Multibeam Echosounders. Ph.D. Thesis, Ghent University, Ghent, Belgium, 2019.
8. Bai, Q.; Mestdagh, S.; Snellen, M.; Simons, D.G. Indications of marine benthos occurrence from multi-spectral multi-beam backscatter data: A case study in the North Sea. *Front. Earth Sci.* **2023**, *11*, 1140649. [CrossRef]
9. Schulze, I.; Gogina, M.; Schönke, M.; Zettler, M.L.; Feldens, P. Seasonal change of multifrequency backscatter in three Baltic Sea habitats. *Front. Remote Sens.* **2022**, *3*, 956994. [CrossRef]
10. Colbo, K.; Ross, T.; Brown, C.; Weber, T. A review of oceanographic applications of water column data from multibeam echosounders. *Estuar. Coast. Shelf Sci.* **2014**, *145*, 41–56. [CrossRef]
11. Koslow, J.A. The role of acoustics in ecosystem-based fishery management. *ICES J. Mar. Sci.* **2009**, *66*, 966–973. [CrossRef]
12. Trenkel, V.; Ressler, P.; Jech, M.; Giannoulaki, M.; Taylor, C. Underwater acoustics for ecosystem-based management: State of the science and proposals for ecosystem indicators. *Mar. Ecol. Prog. Ser.* **2011**, *442*, 285–301. [CrossRef]
13. Benoit-Bird, K.J.; Lawson, G.L. Ecological insights from pelagic habitats acquired using active acoustic techniques. *Annu. Rev. Mar. Sci.* **2016**, *8*, 463–490. [CrossRef]
14. Simmons, S.M.; Parsons, D.R.; Best, J.L.; Oberg, K.A.; Czuba, J.A.; Keevil, G.M. An evaluation of the use of a multibeam echo-sounder for observations of suspended sediment. *Appl. Acoust.* **2017**, *126*, 81–90. [CrossRef]
15. Fromant, G.; Le Dantec, N.; Perrot, Y.; Floc'h, F.; Lebourges-Dhaussy, A.; Delacourt, C. Suspended sediment concentration field quantified from a calibrated MultiBeam EchoSounder. *Appl. Acoust.* **2021**, *180*, 108107. [CrossRef]
16. Weber, T.C.; Mayer, L.; Jerram, K.; Beaudoin, J.; Rzhanov, Y.; Lovalvo, D. Acoustic estimates of methane gas flux from the seabed in a 6000 km^2; region in the Northern Gulf of Mexico. *Geochem. Geophys. Geosyst.* **2014**, *15*, 1911–1925. [CrossRef]
17. Spain, E.; Lamarche, G.; Lucieer, V.; Watson, S.J.; Ladroit, Y.; Heffron, E.; Pallentin, A.; Whittaker, J.M. Acoustic Predictors of Active Fluid Expulsion From a Hydrothermal Vent Field, Offshore Taupō Volcanic Zone, New Zealand. *Front. Earth Sci.* **2022**, *9*, 785396. [CrossRef]

18. Janowski, Ł.; Pydyn, A.; Popek, M.; Gajewski, J.; Gminska-Nowak, B. Towards better differentiation of archaeological objects based on geomorphometric features of a digital elevation model, the case of the Old Oder Canal. *Archaeol. Prospect.* **2024**, 1–12. [CrossRef]
19. Demer, D.A.; Berger, L.; Bernasconi, M.; Bethke, E.; Boswell, K.; Chu, D.; Domokos, R.; Dunford, A.; Fassler, S.; Gauthier, S.; et al. *Calibration of Acoustic Instruments*; ICES Cooperative Research Report No. 326; International Council for the Exploration of the Sea: Copenhagen, Denmark, 2015.
20. Lurton, X.; Lamarche, G. (Eds.) Backscatter Measurements by Seafloor-Mapping Sonars: Guidelines and Recommendations. 2015. Available online: https://zenodo.org/records/10089261 (accessed on 27 March 2024).
21. Eleftherakis, D.; Berger, L.; Le Bouffant, N.; Pacault, A.; Augustin, J.-M.; Lurton, X. Backscatter calibration of high-frequency multibeam echosounder using a reference single-beam system on natural seafloor. *Mar. Geophys. Res.* **2018**, *39*, 55–73. [CrossRef]
22. Roche, M.; Degrendele, K.; Vrignaud, C.; Loyer, S.; Le Bas, T.; Augustin, J.-M.; Lurton, X. Control of the repeatability of high frequency multibeam echosounder backscatter by using natural reference areas. *Mar. Geophys. Res.* **2018**, *39*, 89–104. [CrossRef]
23. Snellen, M.; Gaida, T.C.; Koop, L.; Alevizos, E.; Simons, D.G. Performance of Multibeam Echosounder Backscatter-Based Classification for Monitoring Sediment Distributions Using Multitemporal Large-Scale Ocean Data Sets. *IEEE J. Ocean. Eng.* **2019**, *44*, 142–155. [CrossRef]
24. Applied Physics Laboratory (APL). *APL-UW High-Frequency Ocean Environmental Acoustic Models Handbook*; Technical Report APL-UW TR9407; APL, University of Washington: Seattle, WA, USA, 1994.
25. Gaida, T.C.; Snellen, M.; Van Dijk, T.A.G.P.; Simons, D.G. Geostatistical modelling of multibeam backscatter for full coverage seabed sediment maps. *Hydrobiologia* **2019**, *845*, 55–79. [CrossRef]
26. Gaida, T.C. Acoustic Mapping and Monitoring of the Seabed—From Single-Frequency to Multispectral Multibeam Backscatter. Ph.D. Thesis, Delft University of Technology, Delft, The Netherlands, 2020.
27. Thorne, P.D.; Pace, N.G.; Al-Hamdani, Z.K.S. Laboratory measurements of backscattering from marine sediments. *J. Acoust. Soc. Am.* **1988**, *84*, 303–309. [CrossRef]
28. Parthiot, F.; de Nanteuil, E.; Merlin, F.X.; Zerr, B.; Guedes, Y.; Lurton, X.; Augustin, J.-M.; Cervenka, P.; Marchal, J.; Sessarego, J.P.; et al. Sonar detection and monitoring of sunken heavy fuel oil on the seafloor. In Proceedings of the Interspill 2004 Conference, Trondheim, Norway, 14–17 June 2004.
29. Ivakin, A.N.; Sessarego, J.P. High frequency broad band scattering from water-saturated granular sediments: Scaling effects. *J. Acoust. Soc. Am.* **2007**, *122*, 165–171. [CrossRef]
30. Williams, K.L.; Jackson, D.A.; Tang, D.; Briggs, K.B.; Thorsos, E.I. Acoustic backscattering from a sand and a sand/mud environment: Experiments and data/model comparisons. *IEEE J. Ocean. Eng.* **2009**, *34*, 388–398. [CrossRef]
31. Li, J.; An, W.; Xu, C.; Hu, J.; Gao, H.; Du, W.; Li, X.Y. Sunken oil detection and classification using MBES backscatter data. *Mar. Pollut. Bull.* **2022**, *180*, 113795. [CrossRef] [PubMed]
32. Van Gent, M.R.A. The new Delta Flume for large-scale testing. In Proceedings of the 36th IAHR World Congress, The Hague, The Netherlands, 28 June–3 July 2015.
33. Trenkel, V.M.; Mazauric, V.; Berger, L. The new fisheries multibeam echosounder ME70: Description and expected contribution to fisheries research. *ICES J. Mar. Sci.* **2008**, *65*, 645–655. [CrossRef]
34. Kongsberg EK80 Wide Band Scientific Echo Sounder—Reference Manual—Release 23.6.0, Kongsberg Technical Document 395234/J 2023. Available online: https://www.kongsbergdiscovery.net/ek80/documents.htm (accessed on 14 March 2024).
35. Kongsberg EM2040c Product Specification. Kongsberg Technical Document 2017. Available online: https://www.kongsberg.com/globalassets/maritime/km-products/product-documents/369468_em2040c_product_specification.pdf (accessed on 20 March 2024).
36. Kongsberg Seapath 130 Series Datasheet. Kongsberg Technical Document 2023. Available online: https://www.kongsberg.com/contentassets/c22a596095db4994a5f26ba216b6b968/110-0034148a_datasheet_seapath130_apr23.pdf (accessed on 20 March 2024).
37. AQUAScat 1000S Datasheet. Aquatech Technical Document 2024. Available online: https://www.aquatecgroup.com/images/Datasheets/Aquatec_AQUAscat_1000S_Datasheet.pdf (accessed on 20 March 2024).
38. SIDUS. SS250 Pan & Tilt Device "Deep Blue". SIDUS Technical Document. Available online: https://www.sidus-solutions.com/product/ss250-pan-tilt-device-deep-blue/ (accessed on 20 March 2024).
39. Augustin, J.-M.; Fezzani, R.; Poncelet, C.; Scalabrin, C. *SonarScope Software*; SEANOE: Plouzane, France, 2022. Available online: https://www.seanoe.org/data/00766/87777/ (accessed on 20 March 2024).
40. Urban, P.; Köser, K.; Greinert, J. Processing of multibeam water column image data for automated bubble/seep detection and repeated mapping. *Limnol. Oceanogr. Methods* **2017**, *15*, 1–21. [CrossRef]
41. Thorne, P.D.; Hanes, D.M. A review of acoustic measurement of small-scale sediment processes. *Cont. Shelf Res.* **2002**, *22*, 603–622. [CrossRef]
42. Betteridge, K.F.E.; Thorne, P.D.; Cooke, R.D. Calibrating multi-frequency acoustic backscatter systems for studying near-bed suspended sediment transport processes. *Cont. Shelf Res.* **2008**, *28*, 227–235. [CrossRef]
43. Francois, R.E.; Garrison, G.R. Sound absorption based on ocean measurements. Part I: Pure water and magnesium sulphate contributions. *J Acoust. Soc. Am.* **1982**, *72*, 896–907. [CrossRef]
44. Francois, R.E.; Garrison, G.R. Sound absorption based on ocean measurements. Part II: Boric acid contribution and equation for total absorption. *J. Acoust. Soc. Am.* **1982**, *72*, 1879–1890. [CrossRef]

45. Moate, B.D.; Thorne, P.D. Interpreting acoustic backscatter from suspended sediments of different and mixed mineralogical composition. *Cont. Shelf Res.* **2012**, *46*, 67–82. [CrossRef]
46. Hughes-Clarke, J. Applications of multibeam water column imaging for hydrographic survey. *Hydrogr. J.* **2006**, *120*, 3.
47. Fettweis, M.; Francken, F.; Pison, V.; Van den Eynde, D. Suspended particulate matter dynamics and aggregate sizes in a high turbidity area. *Mar. Geol.* **2006**, *235*, 63–74. [CrossRef]
48. Fettweis, M.; Nechad, B.; Van den Eynde, D. An estimate of the suspended particulate matter (SPM) transport in the southern North Sea using SeaWiFS images, in situ measurements and numerical model results. *Cont. Shelf Res.* **2007**, *27*, 1568–1583. [CrossRef]
49. Jensen, J.H.; Saremi, S.; Jimenez, C.; Hadjioannou, L. Field experimental observations of highly graded sediment plumes. *Mar. Pollut. Bull.* **2015**, *95*, 72–80. [CrossRef] [PubMed]
50. Mills, D.; Kemps, H. *Generation and Release of Sediments by Hydraulic Dredging: A Review*; Report of Theme 2—Project 2.1; The Dredging Science Node, Western Australian Marine Science Institution: Perth, WA, Australia, 2006; 97p.
51. Van Dijk, T.A.G.P.; Roche, M.; Lurton, X.; Fezzani, R.; Simmons, S.M.; Gastauer, S.; Fietzek, P.; Mesdag, C.; Berger, L.; Klein Breteler, M.; et al. Recorded Data with EM2040 MBES, EK80 SBES and Aquascat System during the BSinFlume Feasibility Experiment in the Delta Flume, Deltares, The Netherlands in 2020. SEANOE. 2020. Available online: https://www.seanoe.org/data/00818/93014/ (accessed on 20 March 2024).